Research Square

Preprints are preliminary reports that have not undergone peer review.
They should not be considered conclusive, used to inform clinical practice,
or referenced by the media as validated information.

Structural Brain Network Differences in Asymptomatic Temporomandibular Joint Disc Displacement: An Exploratory Diffusion MRI Pilot Study

Vasil Pekhno

pekhnyo@ukr.net

Shupyk National Healthcare University of Ukraine

Nataliia Savychuk

State Scientific Institution “Center of Innovative Healthcare Technologies”

Roman Sulik

National Healthcare University of Ukraine

Research Article

Keywords: Temporomandibular Joint Disorders, Diffusion Tensor Imaging, Connectome, Neural Pathways, White Matter

Posted Date: September 20th, 2026

DOI: https://doi.org/10.21203/rs.3.rs-10519594/v1

License: This work is licensed under a Creative Commons Attribution 4.0 International License.
Read Full License

Additional Declarations: No competing interests reported.

Abstract

Background

Structural brain-connectome alterations have been described mainly in painful temporomandibular disorders (TMD), whereas it remains uncertain whether asymptomatic TMD-related pathology is accompanied by detectable structural network differences. We hypothesised that asymptomatic TMD would not be associated with diffuse whole-connectome disruption but might show selective differences within cortical-subcortical systems and highly connected network nodes.

Methods

Seventeen participants were included: nine healthy controls and eight participants with asymptomatic TMD. Diffusion MRI tractography-derived connectivity matrices were generated using five complementary parcellations: HCP-MMP, FreeSurferDKT Subcortical, Brainnetome, Cerebellum-SUIT, and a high-resolution brainstem parcellation. End-region matrices constituted the primary connectivity definition, whereas pass-region matrices were used for workflow-sensitivity analysis. Global graph measures, degree-distribution models, predefined cortical and anatomical systems, nodal measures, targeted edges, participation entropy, degree-based hub disruption, false-discovery-rate correction, and leave-one-out analyses were assessed.

Results

Global structural organisation was largely preserved. Weibull models provided the lowest Akaike information criterion for all 63 end-region participant-by-atlas degree distributions and for 80 of 85 pass-region distributions. No atlas-wide global metric survived FDR correction, and participation entropy did not differ significantly between groups. The most consistent atlas-level pattern was observed with FreeSurferDKT Subcortical, where controls showed higher density, non-zero edge count, and mean and median degree (Cliff's δ approximately 0.51–0.53), with concordant directions across both workflows and leave-one-out analyses. HCP-MMP maximum nodal degree was also higher in controls (δ = 0.61, p = 0.038). Exploratory system-level findings favoured controls within the Central Executive/Frontoparietal Network, including median node strength (δ = 0.903, p = 0.0019, q = 0.317), and within the thalamostriatal system, including maximum node strength (δ = 0.833, p = 0.0025, q = 0.350). Negative hub-disruption slopes in HCP-MMP and Brainnetome indicated greater differences among high-degree nodes. The only FDR-significant ROI-level result, higher right-thalamic maximum edge weight in controls, was not leave-one-out stable.

Conclusions

Asymptomatic TMD was characterised by preserved global structural connectome organisation with selective effect-size-level differences in cortical-subcortical connectivity and highly connected cortical nodes. These exploratory findings do not establish white-matter damage or biomarker utility and require confirmation in larger longitudinal cohorts.

Background

Temporomandibular disorders (TMD) comprise a heterogeneous group of conditions affecting the temporomandibular joints, masticatory muscles, and associated craniofacial structures. Their clinical manifestations range from joint sounds and altered mandibular function to persistent orofacial pain and impaired quality of life. However, the relationship between structural temporomandibular joint abnormalities and clinical symptoms is not straightforward. Magnetic resonance imaging may demonstrate disc displacement and altered disc-condyle relationships in individuals without pain or functional complaints [1, 2]. These observations suggest that peripheral joint abnormalities alone do not fully determine the clinical phenotype. Central neural adaptation, compensation, or individual vulnerability may therefore contribute to whether temporomandibular joint pathology remains asymptomatic or becomes clinically manifest [3].

Most neuroimaging research in TMD has focused on patients with chronic pain. Structural and functional MRI studies have reported alterations in regions involved in nociceptive processing, sensorimotor control, affective regulation, and cognitive modulation, including the trigemino-thalamo-cortical pathway, insular and cingulate cortices, prefrontal and sensorimotor regions, basal ganglia, thalamus, and periaqueductal grey [4]. Network-level differences have also been described within the default mode, salience, sensorimotor, and pain-related systems. Collectively, these findings support the involvement of distributed neural systems in painful TMD rather than an exclusively peripheral mechanism. However, substantial heterogeneity in study populations, imaging methods, analytical approaches, and brain parcellation strategies has limited direct comparison and quantitative synthesis across studies [4]. Recent resting-state functional MRI findings further suggest alterations in clustering and local efficiency, supporting the relevance of network-level organisation in painful TMD [5].

Diffusion MRI provides complementary information by enabling in vivo assessment of white-matter microstructure and tractography-derived structural connectivity. Previous studies in patients with chronic TMD have reported abnormalities involving the trigeminal nerves and cerebral white-matter pathways, including callosal, prefrontal, and other regions associated with sensory, cognitive, and affective processing [6, 7]. However, the available evidence has been derived predominantly from symptomatic pain cohorts and has generally focused on individual tracts, diffusion indices, or selected regions of interest. It therefore remains unclear whether distributed structural-connectivity differences can be detected in individuals with asymptomatic TMD-related pathology before persistent pain and its associated psychological and behavioural features become established.

The interpretation of structural-connectome findings depends partly on how the brain is parcellated and how reconstructed streamlines are assigned to anatomical regions. Our recent critical review highlighted that TMD-related neural processes may involve distributed cortical, subcortical, cerebellar, and brainstem systems that cannot be represented comprehensively by a single parcellation [3]. Combining anatomically complementary atlases may therefore improve coverage and help distinguish findings that are reproducible across anatomical scales from those that are specific to a particular parcellation. Atlas

granularity, parcel size, anatomical boundaries, and streamline-to-region assignment rules can influence the number, weight, and topological distribution of reconstructed connections. Brainstem tractography presents additional challenges because of the small dimensions, close spatial arrangement, and complex fibre architecture of its nuclei and pathways [8].

The present exploratory pilot study investigated structural connectome organisation in participants with asymptomatic TMD and healthy controls using five complementary parcellations: HCP-MMP, FreeSurferDKT Subcortical, Brainnetome, Cerebellum-SUIT, and the high-resolution human brainstem atlas developed by Adil et al. End-region matrices constituted the primary connectivity definition, whereas pass-region matrices were used as a workflow-sensitivity analysis. We evaluated degree-distribution characteristics, global graph measures, predefined functional and anatomical systems, nodal and targeted edge measures, participation entropy, and degree-based hub disruption. We hypothesised that asymptomatic TMD would not be associated with diffuse whole-connectome disorganisation but might show selective attenuation within cortical-subcortical systems and highly connected network nodes, particularly within executive/frontoparietal, salience-limbic, thalamostriatal, and pain-modulatory systems.

Methods

Study design and setting

This prospective observational pilot study was conducted at the Shupyk National Healthcare University of Ukraine and the National Children's Specialized Hospital "OHMATDYT", Ministry of Health of Ukraine, Kyiv, Ukraine. Participants were prospectively enrolled between January and March 2025 and underwent clinical assessment and diffusion MRI according to a predefined study protocol. De-identified diffusion MRI datasets and associated clinical variables were analysed within an institutional collaboration agreement.

The study compared participants with asymptomatic temporomandibular disorders (TMD) and healthy controls to investigate between-group differences in structural connectome organisation. It formed part of a registered research and development project in Ukraine (registration No. 0125U003930).

Participants and clinical classification

The analytic sample comprised 17 participants: eight participants with asymptomatic temporomandibular disorder and nine healthy controls. Group classification was based on a standardised clinical examination performed according to the Diagnostic Criteria for Temporomandibular Disorders (DC/TMD), supplemented by temporomandibular joint MRI where available.

Participants were assigned to the asymptomatic TMD group when they reported no TMD-related complaints, had no familiar pain in the temporomandibular joints or masticatory muscles, and had MRI-confirmed disc displacement with reduction in at least one temporomandibular joint. Healthy controls reported no TMD-related complaints, had no DC/TMD-defined painful or non-painful TMD diagnosis, and showed no clinically relevant mandibular dysfunction. TMJ MRI was available for eight of the nine healthy controls and demonstrated normal disc position bilaterally in all eight.

The clinical assessment included a structured history of temporomandibular symptoms and examination of mandibular function, joint sounds, and pain responses. Current TMD-related pain was assessed using the DC/TMD symptom-history and clinical-examination procedures.

Participants were eligible for structural-connectome analysis when complete clinical-classification data and diffusion MRI data suitable for tractography and connectivity-matrix construction were available. Datasets with incomplete clinical information, incomplete diffusion imaging, or technically invalid connectivity matrices were excluded.

Diffusion MRI acquisition

Diffusion MRI data were acquired using a 1.5-T Siemens Aera MRI system (Siemens Healthineers, Erlangen, Germany) with a head-and-neck receive coil. A single-shell diffusion-weighted echo-planar imaging sequence (ep2d_diff_mddw_20_p2) was used.

The acquisition parameters included an echo time of 97 ms, an in-plane resolution of approximately 1.80 × 1.80 mm, a slice thickness of 5 mm, an interslice distance of 6.5 mm, a flip angle of 90°, and a diffusion weighting of b = 1000 s/mm², with additional b = 0 images. Repetition time varied between 4000 and 4700 ms across participants. The protocol contained 20 unique diffusion-encoding directions.

Participants were positioned supine with the head stabilised within the coil and the mandible maintained in a closed-mouth position. They were instructed to minimise head and mandibular movements throughout the diffusion sequence.

Diffusion MRI reconstruction and tractography

Diffusion MRI data were processed using DSI Studio (March 2026). The original DICOM series were converted into DSI Studio source files and reconstructed using the diffusion tensor imaging model. The reconstructed data were resampled to an isotropic spatial resolution of 2.0 mm.

Whole-brain deterministic fibre tracking was performed using fractional anisotropy as the tracking index. Fractional anisotropy was used solely to guide streamline reconstruction and was not analysed as a study outcome. The anisotropy threshold was based on a predefined Otsu-derived threshold-factor range

of 0.5–0.7, and the angular-threshold range was 45°-90°. The tracking step size corresponded to the reconstructed voxel size, and accepted streamline lengths ranged from 30 to 200 mm.

The same DSI Studio reconstruction, deterministic tractography, atlas-assignment, and connectivity-matrix export workflow was applied to all participants. All reconstruction, tracking, streamline-selection, atlas-assignment, and export parameters were held constant across datasets, with no participant-specific adjustment of processing settings. Structural connectivity was quantified using the number of reconstructed streamlines assigned to each pair of anatomical regions.

Anatomical parcellations, connectivity matrices, and quality control

Structural connectivity matrices were generated for five complementary parcellations: the Human Connectome Project Multi-Modal Parcellation (HCP-MMP), FreeSurferDKT Subcortical, Brainnetome, Cerebellum-SUIT, and a 25-region exploratory brainstem parcellation developed with reference to the high-resolution atlas of Adil et al. The HCP-MMP atlas was used for detailed cortical analyses, FreeSurferDKT Subcortical for cortical-subcortical and thalamostriatal analyses, Brainnetome for complementary cross-atlas analyses, Cerebellum-SUIT for cerebellar analyses, and the brainstem parcellation for exploratory brainstem evaluation.

Two streamline-to-region assignment definitions were applied. Under the primary end-region definition, a streamline contributed to an edge when its endpoints were assigned to two anatomical regions. Under the pass-region definition, a streamline contributed to an edge when it traversed the relevant regions, irrespective of endpoint location. Pass-region matrices were used only as a workflow-sensitivity analysis.

Matrics were undirected and weighted by streamline count, with self-connections excluded from graph analyses. Five matrices were generated for each participant under each connectivity definition, yielding 85 end-region and 85 pass-region matrices.

All matrices underwent automated quality control for expected dimensions, ROI labels and ordering, symmetry, missing or invalid values, and negative connectivity weights. All 170 matrices passed quality control and were retained for analysis. The comparatively sparse brainstem matrices were interpreted as exploratory.

Connectome analyses

Anatomical regions were represented as nodes, and non-zero streamline-count connections were represented as edges. Global measures included graph density, number of non-zero edges, mean, median, variability and maximum nodal degree. Nodal degree represented the number of non-zero connections of a node, whereas node strength represented the sum of its streamline-count weights.

Degree distributions were fitted to five candidate models: power law, truncated power law, log-normal, exponential, and Weibull. Model preference was determined using the Akaike information criterion. Distribution fitting was restricted to matrices meeting the prespecified minimum requirements for the number and variability of nodal degree observations.

Network- and system-level analyses examined the Central Executive/Frontoparietal, Salience/Cingulo-Opercular, Limbic/Reward, thalamostriatal, and pain-modulatory systems. Within- and between-system measures included connection density, number of non-zero edges, node strength, edge weight, total strength, and degree, where applicable.

The complete ROI-to-network and ROI-to-system mapping used in these analyses is provided in Supplementary Table S2.

Node-level analyses evaluated degree, strength, and maximum incident edge weight. Edge-level analyses evaluated selected region-to-region connections within the systems of interest. Node- and edge-level findings were treated as exploratory and subjected to multiple-comparison correction.

Participation entropy was calculated as the Shannon entropy of each participant's distribution of degree across the defined networks. Degree-based hub disruption was assessed by regressing the between-group difference in mean nodal degree against the corresponding mean nodal degree in controls. Negative slopes indicated relatively greater degree reductions among nodes that were more highly connected in controls. Rich-club coefficients were not calculated.

Statistical analysis

Continuous connectome measures were compared between groups using two-sided Mann-Whitney U tests. Effect sizes were quantified using Cliff's delta, with positive values indicating higher values in controls and negative values indicating higher values in the asymptomatic TMD group.

False-discovery-rate correction was performed using the Benjamini-Hochberg procedure within analysis-specific comparison families. Unadjusted p values, FDR-adjusted q values, and effect sizes were reported. Statistical significance was defined as a two-sided p or q value below 0.05, as applicable.

Permutation testing was used for selected topology, network, edge, and hub-disruption analyses. Depending on the analysis family, 10,000 permutations were used for global topology measures, 5,000 for network- and edge-level comparisons, and 2,000 for hub-disruption slopes.

Because of the exploratory design and small sample size, interpretation emphasised effect magnitude, FDR-adjusted results, and consistency across sensitivity analyses rather than nominal statistical significance alone.

Sensitivity analyses

The pass-region workflow was used to assess whether findings depended on the streamline-to-region assignment rule. Direction and magnitude of Cliff's delta values were compared between end-region and pass-region analyses, and broader effect-size similarity was assessed using directional agreement and Spearman rank correlation.

Leave-one-out analyses were performed by sequentially excluding each participant and repeating the relevant group comparisons. An additional participant-exclusion analysis was performed for findings that appeared particularly sensitive to a single observation. These analyses were considered supplementary and were not treated as independent replication.

Sample-size considerations

No formal a priori sample-size calculation was performed. The available sample comprised participants who met the clinical classification criteria and had complete diffusion MRI and connectivity-matrix data suitable for analysis.

The study was designed as an exploratory, hypothesis-generating pilot investigation rather than as a confirmatory or biomarker-validation study. The observed effect sizes may inform sample-size planning for future adequately powered investigations.

Ethics approval and consent to participate

The study was conducted in accordance with the Declaration of Helsinki and was approved by the Commission on Ethics and Academic Integrity of the Shupyk National Healthcare University of Ukraine, Kyiv, Ukraine (Protocol No. 13/10, 17 December 2024). It formed part of a registered research and development project in Ukraine (registration No. 0125U003930).

Written informed consent was obtained from all participants and, where applicable, their legal guardians before clinical assessment and MRI examination. De-identified diffusion MRI datasets and associated clinical variables were processed under an institutional collaboration agreement between the participating institutions.

Results

Participant characteristics

In this study were included 17 participants: eight participants with asymptomatic MRI-confirmed TMJ disc displacement and nine healthy controls. The mean age at examination was 19.4 ± 3.1 years in the asymptomatic group and 25.1 ± 10.6 years in the control group. The corresponding median ages were 20 and 21 years, respectively. Age distributions differed between the groups (Mann-Whitney U = 58.5, p = 0.029).

Temporomandibular joint MRI findings

TMJ MRI showed normal disc position bilaterally in all eight healthy controls with available TMJ MRI data. In contrast, disc displacement with reduction was identified in at least one joint in all eight participants in the asymptomatic group. Disc displacement was unilateral in six participants and bilateral in two. In one participant, the right TMJ was classified as disc displacement with reduction with intermittent locking.

Global connectome organization and degree-distribution modelling

Degree-distribution modelling showed broadly preserved global connectome organization in both groups. In the primary end-region workflow, the Weibull distribution provided the lowest-AIC fit for all 63 fitted subject-by-atlas degree distributions. In the pass-region workflow, Weibull was preferred in 80 of 85 distributions, whereas five distributions were better described by a log-normal model. These exceptions involved four matrices from the custom high-resolution human brainstem atlas of Adil et al. (2021) atlas and one Cerebellum-SUIT matrix.

Participant-by-atlas degree distributions, fitted models, and model-selection frequencies are presented in Supplementary Figure S10.

Complete participant-by-atlas degree-distribution fitting results are provided in Supplementary Table S1.

Unfortunatly no FDR-significant between-group differences were identified in the fitted degree-distribution parameters. Thus, asymptomatic TMD was not associated with a fundamental change in the overall form of structural connectome degree distributions. The results instead supported preservation of global topological organization, allowing subsequent analyses to focus on selective atlas-, network-, and node-level connectivity differences.

Global graph measures

Global graph measures showed no evidence of widespread structural connectome disruption in the asymptomatic TMD group. No atlas-wide comparison survived FDR correction, and most global metrics showed small or inconsistent between-group effects.

The most consistent pattern was observed in the FreeSurferDKT Subcortical atlas. Controls demonstrated higher graph density, number of nonzero edges, mean and median nodal degree, and degree variability than participants with asymptomatic TMD. Effect sizes were moderate, with Cliff's δ values of approximately 0.51-0.53, and the direction of the effects was consistent across both end-region and pass-region workflows.

Within the primary HCP-MMP cortical atlas, controls also showed a nominally higher maximum nodal degree than the TMD group (Cliff's δ = 0.61, p = 0.038), together with smaller differences in degree

variability. These findings suggested reduced representation of highly connected cortical nodes rather than a uniform reduction in cortical connectivity. Participant-level distributions of the principal FreeSurferDKT Subcortical and HCP-MMP graph measures are shown in Figure 1.

Figure 1 Participant-level global connectome measures in controls and asymptomatic TMJ disc displacement

Global metrics derived from Brainnetome, Cerebellum-SUIT, and the **custom high-resolution human brainstem atlas of Adil et al. (2021) atlas** were less consistent between the end-region and pass-region workflows. In particular, cerebellar and brainstem estimates were sensitive to the streamline-to-region assignment rule and were therefore not used to support the principal conclusions. Overall, the global analysis indicated selectively lower subcortical connectivity and cortical maximum degree in asymptomatic TMD against a background of largely preserved global graph organization.

Participant-level distributions of global graph measures derived from the end-region and pass-region workflows are presented in Supplementary Figures S1 and S2, respectively. Complete participant- and atlas-level numerical results, including global graph measures, degree-distribution parameters, nodewise analyses, hub-related analyses, and leave-one-out sensitivity results, are provided in Supplementary Table S1

Predefined network- and system-level findings

Predefined network- and system-level analyses identified several directionally coherent effect-size-level patterns favouring higher streamline-count-derived structural connectivity in controls than in participants with asymptomatic TMD. Unfortunaly none of the principal network- or system-level comparisons survived false-discovery-rate correction. These results can be interpreted as exploratory and hypothesis-generating. The absence of FDR significance limits confirmatory inference but does not, by itself, establish the absence of non-zero effect-size-level differences.

Within the HCP-MMP atlas, structural connections among regions assigned to the Central Executive/Frontoparietal Network showed the most prominent cortical network-level pattern. In the primary end-region workflow, median within-system node strength was higher in controls (Cliff's δ = 0.903, Mann-Whitney p = 0.0019, FDR q = 0.317). Congruent differences were observed for within-system density, non-zero edge count, and average non-zero degree (each δ = 0.722, p = 0.014, q = 0.465). Cross-workflow directional agreement across the broader CEN/FPN metric set was approximately 83%, and the median-node-strength contrast retained the same Control > TMD direction in the complementary pass-region sensitivity analysis, although with a smaller effect size.

Within the thalamostriatal system defined using the FreeSurferDKT Subcortical cortical-subcortical parcellation, controls showed higher maximum node strength (δ = 0.833, p = 0.0025, q = 0.350) and higher maximum edge weight (δ = 0.778, p = 0.0081, q = 0.350). Mean edge weight, average node strength, and total strength showed the same direction and large effect sizes. None of these

comparisons survived FDR correction. Across the broader thalamostriatal metric set, cross-workflow directional agreement was approximately 60%; however, the two headline strength- and weight-based contrasts reversed direction in the pass-region workflow. The end-region pattern was therefore treated as an exploratory anatomical system-level candidate rather than a workflow-robust finding.

As a secondary between-system comparison in HCP-MMP, mean non-zero edge weight between the Limbic/Reward Network and the Salience/Cingulo-Opercular Network was higher in controls (δ = 0.778, Mann-Whitney p = 0.0055, q = 0.458). A permutation-based sensitivity analysis produced p = 0.020. The same Control > TMD direction was observed in the pass-region workflow, but with a smaller effect size and without nominal significance. This salience-limbic structural connectivity contrast was therefore regarded as secondary and less stable than the CEN/FPN pattern. The broader distribution of within-network median-degree effects across anatomical parcellations is presented in Supplementary Figure S9.

Taken together, the CEN/FPN showed the most conspicuous cortical network-level effect-size pattern, the thalamostriatal system represented the principal anatomical system-level candidate, and salience-limbic between-system connectivity provided a secondary exploratory signal. None of these findings was confirmatory, and none constituted biomarker evidence. The broader distribution of within-network median-degree effects across anatomical parcellations is presented in Supplementary Figure S9.

Complete network- and system-level comparisons, including end-region and pass-region results, are provided in Supplementary Table S2.

Subcortical connectivity findings

The FreeSurferDKT Subcortical atlas showed the most consistent localized between-group pattern. Compared with participants with asymptomatic TMD, controls had more nonzero edges, greater graph density, and higher mean and median nodal degree, with moderate effect sizes of approximately Cliff's δ = 0.51-0.53. These differences did not survive FDR correction but showed the same direction in the end-region and pass-region workflows and remained directionally stable across all leave-one-out iterations.

Within the thalamostriatal system, controls showed higher maximum node strength (Cliff's δ = 0.833, p = 0.0025, q = 0.350) and higher maximum edge weight (δ = 0.778, p = 0.0081, q = 0.350). Higher mean edge weight, average node strength, and total strength were observed in the same direction. Because these findings did not survive FDR correction and were weaker in the pass-region workflow, they were interpreted as exploratory evidence of thalamostriatal attenuation.

At the node level, the right thalamus proper showed higher maximum edge weight in controls in the primary end-region analysis (Cliff's δ = 0.944, p = 0.000329, q = 0.02962). However, this was the only ROI-level finding to survive FDR correction and lost significance after exclusion of one participant. It was therefore treated as sensitivity-dependent and not as a confirmatory standalone result.

Hub-disruption and high-degree node analysis

Hub-disruption regression demonstrated a preferential reduction of connectivity in high-degree nodes in the asymptomatic TMD group. In the primary end-region workflow, the relationship between the group difference in nodal degree and the mean control-group degree was negative for HCP-MMP (slope = −0.179, R^2 = 0.21, permutation p = 0.0005) and Brainnetome (slope = −0.160, R^2 = 0.17, permutation p = 0.0005). A weaker negative association was also observed for FreeSurferDKT Subcortical (slope = −0.184, p = 0.040).

The negative slopes indicated that nodes with the highest mean degree in controls tended to show the greatest relative degree reductions in participants with asymptomatic TMD, whereas lower-degree nodes were comparatively preserved. The HCP-MMP and Brainnetome patterns were reproduced in the pass-region workflow, supporting consistency across the two streamline-to-region assignment definitions.

Degree-based hub-disruption patterns for the principal cortical parcellations are shown in Figure 2.

Figure 2 Degree-based hub-disruption patterns in HCP-MMP and Brainnetome parcellations

Consistent with this pattern, maximum nodal degree in the HCP-MMP atlas was lower in the TMD group, with a large nominal effect (Cliff's δ = 0.61, p = 0.038). Taken together, these findings suggested preferential attenuation of high-degree cortical nodes rather than uniform loss of connectivity throughout the connectome. Because rich-club coefficients were not directly calculated, these results were interpreted specifically as **degree-based hub disruption** and not as evidence of rich-club disruption.

Targeted edge-level findings

The targeted exploratory analysis included 6,580 predefined ROI-to-ROI connections selected from the CEN/FPN, salience-limbic, thalamostriatal, and Brainnetome sensitivity systems. Forty connections reached nominal significance, but none survived FDR correction. The distribution of nominally significant targeted edge-level comparisons is presented in Supplementary Figure S7. None of these connections survived false-discovery-rate correction.

Within the HCP-MMP CEN/FPN, the largest effects favored controls for the R_7PL-R_a47r and R_44-R_TE1m connections (both Cliff's δ = 0.667, p ≈ 0.008), followed by R_44-R_p9-46v (δ = 0.625, p = 0.025) and L_PGp-L_IP0 (δ = 0.556, p = 0.020). In the subcortical analysis, the right thalamus proper-right caudate connection was also stronger in controls (δ = 0.778, p = 0.008), consistent with the broader thalamostriatal pattern.

After exclusion of the principal outlier, the number of nominal findings decreased from 40 to 21. Four CEN/FPN connections, including R_7PL-R_a47r, R_44-R_TE1m, R_44-R_p9-46v, and L_PGp-L_IP0, remained nominally stable, as did the right thalamus proper-right caudate connection. Because no edge

survived FDR correction in either analysis, these findings were interpreted as hypothesis-generating localization of the network/system-level pattern rather than confirmatory edge-level effects.

Participation entropy and network integration

Participation entropy did not differ meaningfully between the control and asymptomatic TMD groups across any of the five atlases or either streamline-assignment workflow. All effects were small to moderate and statistically non-significant, with absolute Cliff's δ values not exceeding 0.39 and p values ≥ 0.11. The largest effect was observed in the end-region FreeSurferDKT Subcortical analysis but remained non-significant.

The preserved participation entropy indicated that the overall diversity with which nodes distributed their connections across predefined systems was maintained in asymptomatic TMD. This finding was consistent across the HCP-MMP, Brainnetome, FreeSurferDKT Subcortical, Cerebellum-SUIT, and **custom high-resolution human brainstem atlas of Adil et al. (2021) atlas** analyses.

Thus, the selective reductions observed in CEN/FPN, salience-limbic, and thalamostriatal connectivity were not accompanied by a global redistribution of network participation. Together with the preserved degree-distribution form, this supported maintained large-scale connectome organization despite localized attenuation of connectivity strength and high-degree nodes. Participant-level participation-entropy values for the Brainnetome and HCP-MMP parcellations are presented in Supplementary Figure S8.

Robustness and sensitivity analyses

Comparison of the end-region and pass-region workflows identified 18 metrics with the same direction and at least moderate effect magnitude under both streamline-to-region assignment definitions. The most stable pattern involved the FreeSurferDKT Subcortical atlas: graph density, number of nonzero edges, and mean nodal degree were consistently higher in controls and retained the same direction in all 17 leave-one-out iterations. The corresponding cross-atlas effect profiles showed a Spearman correlation of 0.56 and 80% directional agreement. The correspondence of atlas-level effect sizes between the end-region and pass-region workflows is shown in Supplementary Figure S3. Leave-one-out stability of the principal FreeSurferDKT Subcortical and HCP-MMP global graph findings is presented in Supplementary Figure S5.

The reduction in HCP-MMP maximum nodal degree was also directionally stable across all leave-one-out iterations. Hub-disruption slopes remained negative in both workflows for HCP-MMP and Brainnetome, with permutation p = 0.0005, supporting preferential attenuation of highly connected cortical nodes. Interesting was that Salience-limbic coupling showed identical effect magnitude and direction in both workflows, whereas CEN/FPN metrics demonstrated approximately 83% directional agreement.

Cross-atlas similarities and differences in the between-group effect-size profiles are presented in Supplementary Figure S4.

Thalamostriatal findings showed only partial cross-workflow agreement, with approximately 60% directional stability. But the FDR-significant right-thalamic maximum edge-weight finding from the end-region analysis did not remain significant after leave-one-out exclusion and was not reproduced as the leading pass-region effect. It was therefore considered participant-sensitive rather than confirmatory. The participant-level distribution of the right thalamus proper maximum edge-weight finding is shown in Supplementary Figure S6.

Cerebellum-SUIT global metrics, several Brainnetome global measures, and results derived from the **custom high-resolution human brainstem atlas of Adil et al. (2021) atlas** changed direction or magnitude between workflows. Brainstem findings were additionally affected by sparse matrices and individual outliers. These results were classified as workflow-sensitive and were not used to support the principal biological interpretation.

Detailed cross-workflow, cross-atlas, and leave-one-out sensitivity results are provided in Supplementary Tables S1 and S2.

Integrated summary of structural connectome findings

Taken together, the analyses indicated broadly preserved global structural connectome organization in asymptomatic TMD, accompanied by selective attenuation at the subcortical and high-degree cortical levels. Degree-distribution form, participation entropy, and most whole-connectome measures were comparable between groups, providing no evidence of diffuse network-wide dysconnectivity.

The most reproducible effect-size-level pattern involved lower subcortical connectivity in the FreeSurferDKT Subcortical atlas and preferential attenuation of highly connected cortical nodes. Negative hub-disruption slopes in HCP-MMP and Brainnetome were reproduced across both end-region and pass-region workflows, while subcortical density and degree effects remained directionally stable in all leave-one-out iterations.

Additional exploratory findings localized this pattern to the Central Executive/Frontoparietal Network, salience-limbic coupling, and thalamostriatal connectivity. However, these network- and edge-level effects did not survive FDR correction. The only FDR-significant result, higher right-thalamic maximum edge weight in controls, was not stable under leave-one-out analysis and was therefore not considered confirmatory. The direction and magnitude of the principal atlas-, network-, system-, and node-level between-group effects are summarised in Figure 3.

Figure 3 Principal between-group effect sizes across connectome analyses

Results from Cerebellum-SUIT and the **custom high-resolution human brainstem atlas of Adil et al. (2021) atlas** were workflow-sensitive or affected by matrix sparsity and were not incorporated into the principal interpretation. Overall, the findings supported a model of **selective, effect-size-level attenuation superimposed on preserved global structural organization,** rather than diffuse connectome disruption.

No individual connectivity metric demonstrated sufficient correction-supported and leave-one-out-stable performance to be interpreted as a diagnostic or prognostic biomarker.

Discussion

The principal finding of this exploratory study was that asymptomatic temporomandibular disorder was accompanied by largely preserved global structural connectome organisation rather than diffuse network reorganisation. No atlas-wide global metric remained significant after false-discovery-rate correction, and participation entropy was broadly comparable between groups. Against this stable global background, the most consistent effect-size-level differences involved cortical-subcortical connectome measures derived using the FreeSurferDKT Subcortical parcellation and degree-based differences concentrated among highly connected cortical nodes. Thalamostriatal pathways and structural connections among regions assigned to the Central Executive/Frontoparietal Network emerged as additional hypothesis-generating targets. Overall, the results indicate selective differences in reconstructed connection number, degree, and nodal hierarchy rather than widespread disruption of global network organisation.

The relative preservation of whole-brain organisation partially aligns with the systematic review and meta-analysis by Butry et al. [9], which found low- to very-low-certainty evidence for consistent global structural network abnormalities across chronic pain conditions. However, the present participants had asymptomatic TMD rather than established chronic pain, and this comparison should therefore not be interpreted as evidence of an identical neurobiological phenotype. Moreover, the absence of widespread effects does not exclude subtle structural differences. The field strength and spatial resolution of the diffusion acquisition may have limited sensitivity to small or anatomically complex pathways. Thus, the global findings constrain the likely extent of the observed differences but do not demonstrate complete structural equivalence between groups.

Degree-distribution modelling provided additional evidence that the broad organisational pattern was similar between groups. The Weibull model showed the lowest Akaike information criterion for all end-region participant-by-atlas distributions and for 80 of 85 pass-region distributions, with the remaining five favouring a log-normal model. This consistency suggests that the groups largely retained the same broad family of degree distributions despite regional differences in reconstructed connectivity. It is compatible with previous graph-theoretical studies showing that human structural networks maintain non-random and hierarchically organised properties [10-12]. Nevertheless, similarity in the best-fitting degree distribution does not establish equivalence of the complete network topology, because networks

with comparable degree distributions may still differ in modular organisation, spatial configuration, or nodal connectivity.

The most reproducible atlas-level findings were observed with the FreeSurferDKT Subcortical parcellation. Controls showed higher graph density, a greater number of non-zero edges, and higher mean and median degree, with moderate effect sizes. These effects were directionally consistent across end-region and pass-region connectivity definitions and remained stable in leave-one-out analyses, although they did not survive FDR correction. This pattern partially agrees with diffusion MRI studies in painful TMD reporting differences in the trigeminal nerve and cerebral white-matter pathways involved in sensory, cognitive, and affective processing [6,7], as well as with broader evidence implicating thalamic, basal ganglia, and limbic regions in symptomatic TMD [4]. Direct equivalence is not warranted, however, because the present measures were derived from reconstructed streamline counts rather than tract-specific fractional anisotropy or other microstructural indices. The findings are therefore best interpreted as exploratory differences in cortical-subcortical connectome measures, not as evidence of axonal loss, demyelination, or direct white-matter damage.

Within this broader pattern, the thalamostriatal system emerged as a principal target for further study. Controls showed higher maximum node strength and maximum edge weight in the primary end-region analysis, with large effect sizes, although these comparisons did not remain significant after FDR correction. Maximum edge weight of the right thalamus proper was the only node-level result to survive FDR correction in the full cohort. However, it lost significance during leave-one-out analysis and was not the leading region under the pass-region definition. It should therefore be considered preliminary rather than diagnostic. Its convergence with the broader thalamostriatal pattern and a nominal right thalamus-right caudate edge nevertheless supports targeted investigation of thalamic and striatal pathways. This interpretation partially agrees with literature implicating trigemino-thalamo-cortical and basal ganglia circuits in symptomatic TMD [4,6,7,13,14], but the present data do not demonstrate altered relay function or show that these differences precede pain development.

The most prominent cortical network-level pattern involved structural connections among regions assigned to the Central Executive/Frontoparietal Network. Controls showed higher median within-network node strength, with a large effect size, together with nominal differences in density and degree. Several targeted frontoparietal edges showed the same directional pattern, but none of these comparisons survived FDR correction. Previous studies have implicated executive and frontoparietal networks in chronic pain and symptomatic TMD [15-17]. The present findings are only partially concordant with that literature because they concern reconstructed structural connections in an asymptomatic cohort rather than functional activation or executive performance. The CEN/FPN should therefore be regarded as a candidate cortical system for future investigation, not as an established site of functional impairment.

A less stable result involved structural connectivity between regions assigned to the salience and limbic systems. Mean non-zero edge weight was higher in controls and the primary permutation result was

nominally significant, but the finding did not survive FDR correction and was sensitive to analytical specification. It is conceptually consistent with evidence that salience and limbic systems participate in the sensory, affective, and cognitive dimensions of pain [15,16]. However, the present analysis did not assess functional coupling or pain-related neural activity. This result should therefore remain secondary and requires confirmation in a larger independent cohort.

Degree-based hub-disruption analysis indicated that between-group differences were more pronounced among nodes with high degree in controls. Negative hub-disruption slopes were observed in the HCP-MMP, Brainnetome, and FreeSurferDKT Subcortical parcellations, with directionally consistent HCP-MMP and Brainnetome patterns in the pass-region workflow. Highly connected nodes contribute substantially to distributed communication and integration [10,18], making this pattern potentially relevant to the organisation of cortical-subcortical information transfer. However, the result may partly reflect the lower overall number or density of reconstructed connections, because high-degree nodes provide more potential edges over which group differences can accumulate. The analysis did not directly assess rich-club organisation and does not demonstrate selective hub damage. It is more cautiously interpreted as a directionally consistent degree-based pattern superimposed on largely preserved global organisation.

Comparison of end-region and pass-region workflows served as an analytical sensitivity test. Eighteen metrics showed the same direction and at least moderate effect sizes under both connectivity definitions, while cross-atlas effect profiles demonstrated moderate correlation and approximately 80% directional agreement. The strongest overlap involved FreeSurferDKT Subcortical measures and degree-based patterns, whereas thalamostriatal findings showed only partial agreement. This convergence reduces the likelihood that the main findings were entirely dependent on a single streamline-to-region assignment rule. Nevertheless, both workflows used the same participants, diffusion data, tractography reconstruction, and atlas definitions. Their agreement therefore indicates analytical robustness rather than independent replication.

The multi-atlas design demonstrated that the observed effect profiles depended on anatomical scale and parcellation strategy. FreeSurferDKT Subcortical yielded the most consistent cortical-subcortical effect-size pattern, whereas HCP-MMP and Brainnetome better captured degree-based findings among highly connected cortical nodes. Such atlas dependence may reflect complementary levels of structural organisation, but it may also arise from differences in parcel number, size, anatomical boundaries, and streamline assignment. Convergence across parcellations strengthens shared findings, whereas atlas-specific effects should remain anatomically framed and hypothesis-generating.

Results obtained using Cerebellum-SUIT and the custom high-resolution human brainstem parcellation based on Adil et al. (2021)[19] were less stable across workflows and more sensitive to sparse reconstructed connections and individual observations. They cannot be regarded as reliable evidence of group-level cerebellar or brainstem differences. However, this instability does not exclude biological involvement. Both regions contribute to trigeminal sensory processing, sensorimotor coordination, and orofacial regulation. Their small size, complex fibre architecture, and the spatial resolution of the present

acquisition may have reduced tractography sensitivity. Brainstem and cerebellar connectivity therefore remain relevant targets for studies using larger cohorts, higher-resolution diffusion imaging, and region-specific reconstruction strategies.

Taken together, the findings suggest that asymptomatic TMD may involve selective structural connectome differences without the broad network pattern commonly associated with established chronic pain. The absence of a clear default-mode or wider conventional pain-network signature may reflect the limited clinical expression of the condition, although it cannot establish a distinct disease stage. One hypothesis is that thalamostriatal and CEN/FPN differences represent limited components of network variation that may help distinguish persistent asymptomatic dysfunction from painful TMD. Alternative explanations include adaptation to altered temporomandibular function, pre-existing interindividual variation, or methodological sensitivity to particular anatomical systems. The cross-sectional design cannot determine which explanation is correct or whether any participant will subsequently develop pain.

The present results do not support the clinical use of any ROI, edge, or graph metric as a diagnostic biomarker. Their practical value lies in identifying anatomically defined systems for more focused investigation, particularly thalamostriatal pathways, cortical-subcortical connections, and highly connected frontoparietal nodes. A logical next step would be a separate network-informed tractography and tractometry study examining predefined white-matter pathways selected from these regions. Such research should use larger cohorts, higher-resolution preferably multi-shell diffusion acquisition, advanced fibre-orientation modelling, and prospectively defined tract-specific measures. Integration with functional MRI, neurophysiological assessment, clinical phenotyping, and molecular research may also clarify mechanisms that distinguish asymptomatic joint dysfunction from painful TMD. If confirmed, these systems may inform future mechanism-based therapeutic and pharmacological research, although the current study does not identify treatment targets.

Strengths and limitations

This study has several strengths, including the use of multiple anatomically complementary parcellations, two definitions of streamline-to-region assignment, effect-size-based interpretation, leave-one-out analyses, and explicit correction for multiple comparisons. Nevertheless, the findings should be considered in the context of important limitations. First, the small sample size reduced statistical power and increased the influence of individual observations, particularly in node- and edge-level analyses. Most observed effects did not survive FDR correction and should therefore be regarded as hypothesis-generating. Second, the cross-sectional design cannot determine whether the identified connectivity pattern preceded temporomandibular dysfunction, developed as an adaptation to altered joint function, or represented stable interindividual variation. It also cannot establish whether any participants will subsequently develop painful TMD. Third, the technical characteristics of the 1.5-T single-shell diffusion acquisition and its spatial resolution may have limited sensitivity to subtle or anatomically complex white-matter differences, particularly within the brainstem and cerebellum. Deterministic tractography

and streamline-count-derived edge weights are also influenced by reconstruction parameters, fibre geometry, and parcellation boundaries and should not be interpreted as direct measures of axonal number, tissue integrity, or anatomical connection strength. Finally, agreement between the end-region and pass-region workflows represents analytical robustness within the same dataset rather than independent replication. Larger longitudinal studies using higher-resolution multi-shell diffusion imaging and independent cohorts are required to confirm the present findings.

Conclusion

In this exploratory pilot sample, no evidence of diffuse between-group differences in global structural connectome measures was identified. Exploratory analyses showed directionally lower streamline-count-derived measures in the FreeSurferDKT Subcortical parcellation and between-group differences concentrated among cortical nodes with higher degree in controls. The thalamostriatal and Central Executive/Frontoparietal Network findings represent hypothesis-generating candidate signals, whereas the salience–limbic result was less stable. Most network- and system-level findings did not survive false-discovery-rate correction, and the only FDR-significant ROI-level result was not stable in leave-one-out analysis. Given the small sample, age imbalance, cross-sectional design, and dependence of tractography-derived measures on analytical choices, these findings should not be interpreted as TMD-specific neural alterations, biomarkers, or evidence of white-matter damage. Larger age-balanced longitudinal studies are required to determine whether these patterns are reproducible and clinically relevant.

Abbreviations

AIC - Akaike information criterion;

CCDF - complementary cumulative distribution function;

CEN/FPN - Central Executive/Frontoparietal Network;

DC/TMD - Diagnostic Criteria for Temporomandibular Disorders;

DICOM - Digital Imaging and Communications in Medicine;

DTI - diffusion tensor imaging;

FA - fractional anisotropy;

FDR - false discovery rate;

HC - healthy control;

HCP-MMP - Human Connectome Project Multi-Modal Parcellation;

IQR - interquartile range;

LOO - leave-one-out;

MRI - magnetic resonance imaging;

ROI - region of interest;

SD - standard deviation;

SUIT - Spatially Unbiased Infratentorial Template;

TE - echo time;

TMD - temporomandibular disorder;

TMJ - temporomandibular joint;

TR - repetition time;

δ - Cliff's delta.

Declarations

Use of software and generative AI:

DSI Studio (March 2026) was used for diffusion MRI reconstruction, deterministic tractography, atlas-based streamline assignment, and structural connectivity matrix generation. Cursor (Anysphere, Inc.) was used as an AI-assisted coding environment to develop and execute author-directed scripts for processing and organising the original exported files and derived analytical outputs. OpenAI's ChatGPT was used solely to improve the grammar, punctuation, and readability of text originally written by the authors and to assist in drafting prompts for use in Cursor. All prompts, scripts, analytical outputs, and language revisions were critically reviewed and verified by the authors. All scientific, methodological, and interpretive decisions were made by the authors, who take full responsibility for the final manuscript.

Ethics approval and consent to participate:

The study was conducted in accordance with the Declaration of Helsinki and was approved by the Commission on Ethics and Academic Integrity of the Shupyk National Healthcare University of Ukraine, Kyiv, Ukraine (Protocol No. 13/10, 17 December 2024). Registration card number for Research and Development in Ukraine - 0125U003930. Written informed consent was obtained from all participants and, where applicable, their legal guardians before clinical assessment and MRI examination.

Consent for publication:

Written informed consent for publication of de-identified data was obtained from all participants.

Availability of data and materials:

The de-identified derived datasets supporting the conclusions of this article are included in the article and its supplementary materials.

Supplementary Tables S1 and S2 contain participant-level, atlas-level, network-level, and sensitivity-analysis results. The raw diffusion MRI data and original clinical records are not publicly available because of participant-privacy, ethical, and institutional data-protection restrictions. Additional de-identified structural-connectivity matrices and supporting metadata may be made available by the corresponding author on reasonable request, subject to approval by the participating institutions and compliance with the applicable ethical and data-protection requirements.

Competing interests:

The authors declare that they have no competing interests.

Funding:

This research received no specific grant from any funding agency in the public, commercial, or not-for-profit sectors. The study and preparation of the manuscript were conducted using the institutional resources available to the participating authors and institutions

Authors' contributions:

V.V.P.: Conceptualization; Methodology; Investigation; Data curation; Formal analysis; Software; Visualization; Writing - original draft; Project administration.

N.O.S.: Methodology; Supervision; Validation; Writing - review and editing.

R.V.S.: Methodology; Validation; Neurological interpretation; Writing - review and editing.

Acknowledgements:

Not applicable

References

1. Luo D, Yang Z, Qiu C, Jiang Y, Zhou R, Yang J. A magnetic resonance imaging study on the temporomandibular joint disc-condyle relationship in young asymptomatic adults. Int J Oral Maxillofac Surg. 2022;51(2):226–33. 10.1016/j.ijom.2021.06.010.
2. Maizlin ZV, Nutiu N, Dent PB, Vos PM, Fenton DM, Kirby JM, et al. Displacement of the temporomandibular joint disk: correlation between clinical findings and MRI characteristics. J Can

Dent Assoc. 2010;76:a3.

3. Savychuk N, Pekhno V, Liakhovska A, Sulik R, Riabko I. Brain parcellation for TMD neuroimaging: a critical narrative review. BDJ Open. 2026;12(1):39. 10.1038/s41405-026-00407-2.
4. Yin Y, He S, Xu J, You W, Li Q, Long J, et al. The neuro-pathophysiology of temporomandibular disorders-related pain: a systematic review of structural and functional MRI studies. J Headache Pain. 2020;21(1):78. 10.1186/s10194-020-01131-4.
5. Jiang Y, Li X, Liu M, Chen Z. Investigating changes of functional brain networks in painful temporomandibular disorders: a resting-state fMRI study. J Oral Facial Pain Headache. 2026;40(1):61–70. 10.22514/jofph.2026.006.
6. Moayedi M, Weissman-Fogel I, Salomons TV, Crawley AP, Goldberg MB, Freeman BV, et al. White matter brain and trigeminal nerve abnormalities in temporomandibular disorder. Pain. 2012;153(7):1467–77. 10.1016/j.pain.2012.04.003.
7. Budd AS, Huynh TKT, Seres P, Beaulieu C, Armijo-Olivo S, Cummine J. White matter diffusion properties in chronic temporomandibular disorders: an exploratory analysis. Front Pain Res (Lausanne). 2022;3:880831. 10.3389/fpain.2022.880831.
8. Zhang Y, Furst AJ. Brainstem diffusion tensor tractography and clinical applications in pain. Front Pain Res (Lausanne). 2022;3:840328. 10.3389/fpain.2022.840328.
9. Butry L, Thomä J, Elsenbruch S, Icenhour A, Rehmann R, Enax-Krumova E, et al. Brain network properties in chronic pain: a systematic review and meta-analysis of graph-based connectivity metrics. Front Neurosci. 2025;19:1672542. 10.3389/fnins.2025.1672542.
10. Achard S, Delon-Martin C, Vértes PE, Renard F, Schenck M, Schneider F, et al. Hubs of brain functional networks are radically reorganized in comatose patients. Proc Natl Acad Sci U S A. 2012;109(50):20608–13. 10.1073/pnas.1208933109.
11. Termenon M, Achard S, Jaillard A, Delon-Martin C. The Hub Disruption Index, a reliable index sensitive to the brain networks reorganization: a study of the contralesional hemisphere in stroke. Front Comput Neurosci. 2016;10:84. 10.3389/fncom.2016.00084.
12. Achard S, Salvador R, Whitcher B, Suckling J, Bullmore E. A resilient, low-frequency, small-world human brain functional network with highly connected association cortical hubs. J Neurosci. 2006;26(1):63–72. 10.1523/JNEUROSCI.3874-05.2006.
13. Wilcox SL, Gustin SM, Macey PM, Peck CC, Murray GM, Henderson LA. Anatomical changes within the medullary dorsal horn in chronic temporomandibular disorder pain. NeuroImage. 2015;117:258–66. 10.1016/j.neuroimage.2015.05.014.
14. Cheng X, Li X, Chen J, Qin X, Kang K, Zhang T, et al. Assessing the causal role of the structural connectome in temporomandibular disorders: a Mendelian randomization study. Cranio. 2025;43(6):1053–63. 10.1080/08869634.2024.2419866.
15. Menon V. Large-scale brain networks and psychopathology: a unifying triple network model. Trends Cogn Sci. 2011;15(10):483–506. 10.1016/j.tics.2011.08.003.

16. De Ridder D, Vanneste S, Smith M, Adhia D. Pain and the triple network model. Front Neurol. 2022;13:757241. 10.3389/fneur.2022.757241.
17. Zhao R, Ye Z, Lv X, Li Z, Xiong X. Imaging brain networks: insights into mechanisms of temporomandibular disorders. J Dent Res. 2025;104(4):380–8. 10.1177/00220345241302046.
18. van den Heuvel MP, Sporns O. Rich-club organization of the human connectome. J Neurosci. 2011;31(44):15775–86. 10.1523/JNEUROSCI.3539-11.2011.
19. Adil SM, Calabrese E, Charalambous LT, Cook JJ, Rahimpour S, Atik AF, et al. A high-resolution interactive atlas of the human brainstem using magnetic resonance imaging. NeuroImage. 2021;237:118135. 10.1016/j.neuroimage.2021.118135.

Figures

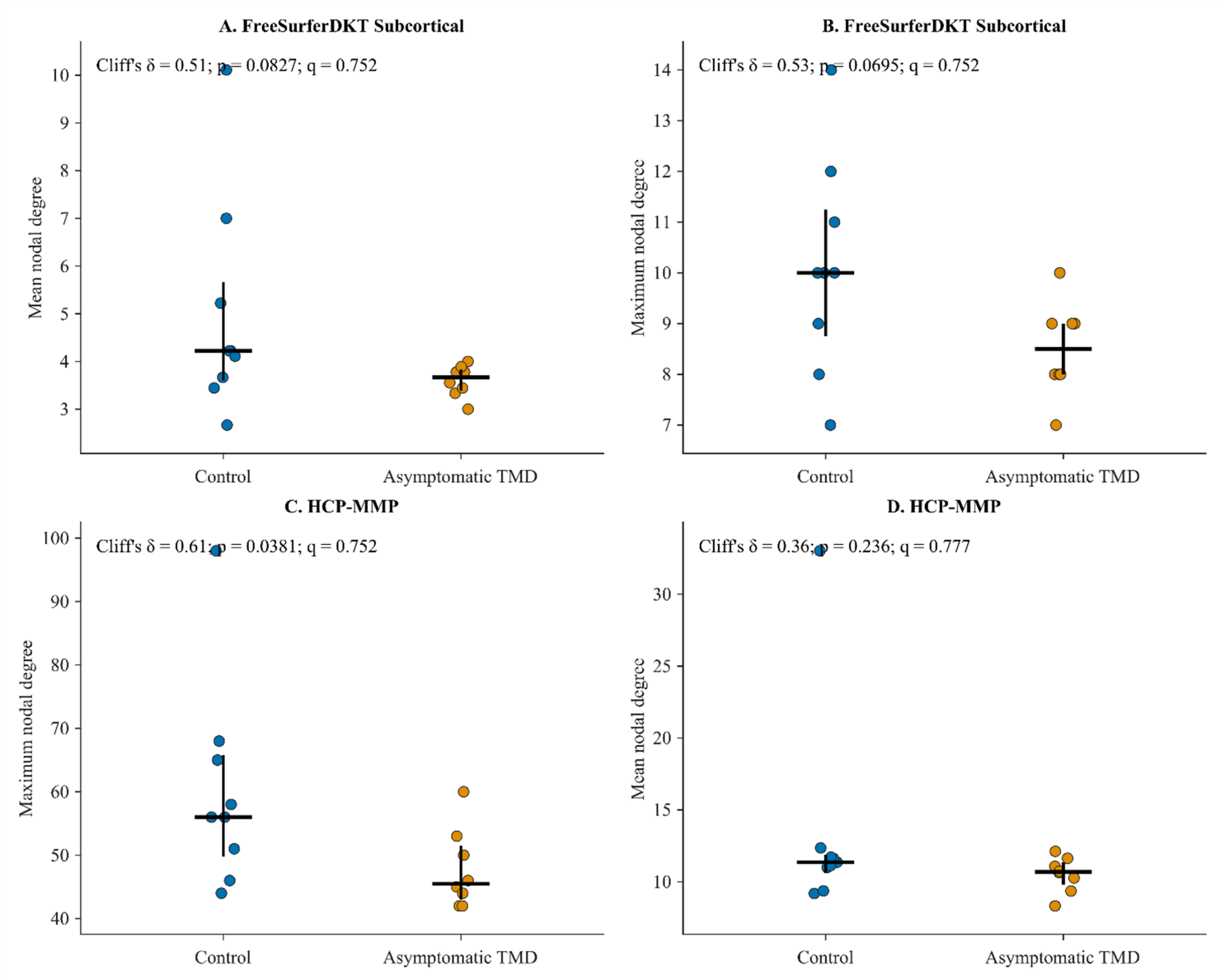


Figure 1

Participant-level global connectome measures in controls and asymptomatic TMJ disc displacement.

Participant-level distributions of selected global graph measures derived from the primary end-region connectivity workflow. (A) Mean nodal degree and (B) maximum nodal degree for the FreeSurferDKT Subcortical parcellation. (C) Maximum nodal degree and (D) mean nodal degree for HCP-MMP. Each point represents one participant; blue points indicate healthy controls and orange points indicate participants with asymptomatic temporomandibular disorder. Horizontal black lines show group medians, and vertical black bars show interquartile ranges. Panel annotations report Cliff's δ, two-sided Mann-Whitney U-test p values, and Benjamini-Hochberg false-discovery-rate-adjusted q values. Positive Cliff's δ values indicate higher measures in controls.

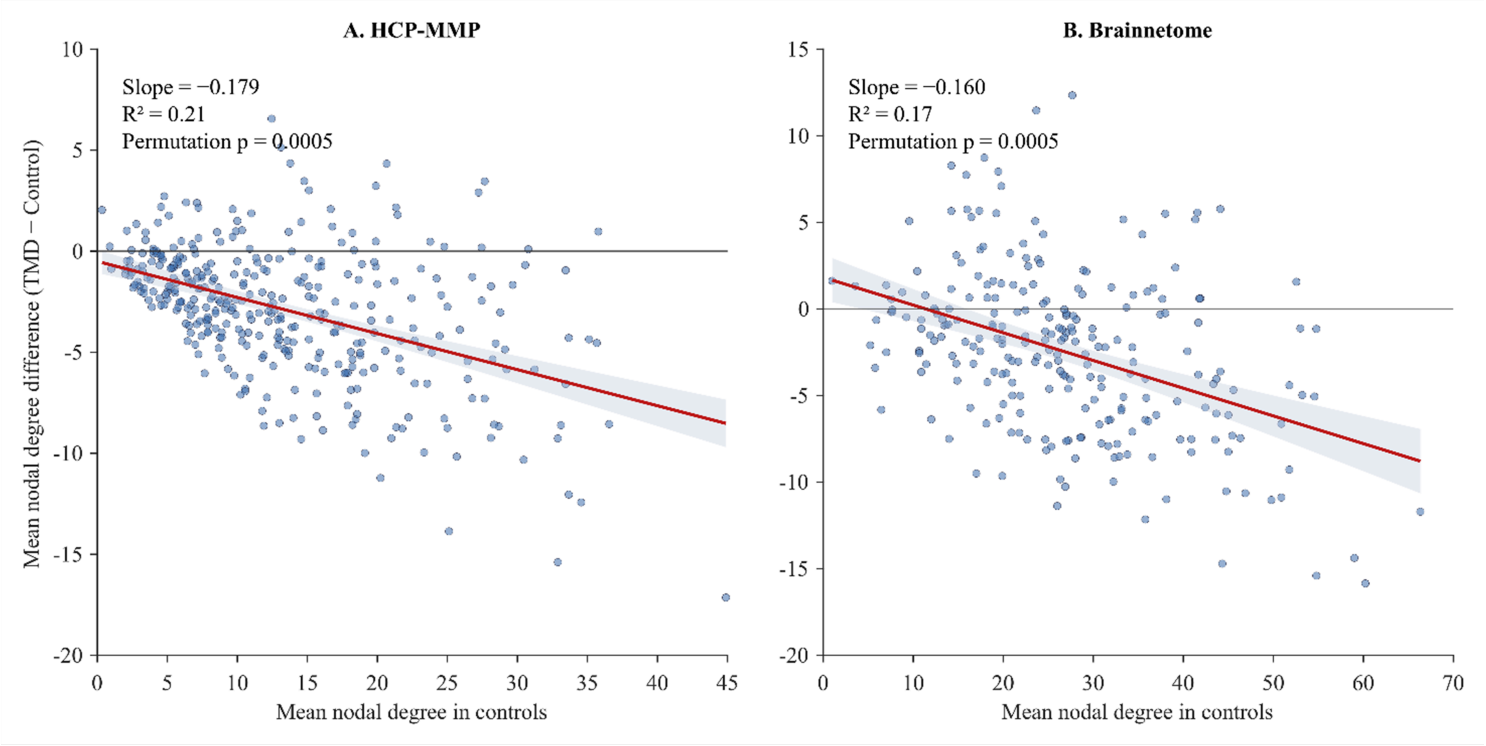


Figure 2

Degree-based hub-disruption patterns in HCP-MMP and Brainnetome.

Degree-based hub-disruption regressions for (A) HCP-MMP and (B) Brainnetome using the primary end-region workflow. Each point represents one atlas node. The x-axis shows mean nodal degree in controls, and the y-axis shows the corresponding between-group difference calculated as TMD minus Control. Red lines show fitted linear regressions, shaded areas show 95% confidence intervals, and horizontal lines denote zero between-group difference. Negative slopes indicate that nodes with higher degree in controls tended to show larger degree reductions in participants with asymptomatic temporomandibular disorder. Regression slopes, coefficients of determination, and permutation-based p values are shown within each panel.

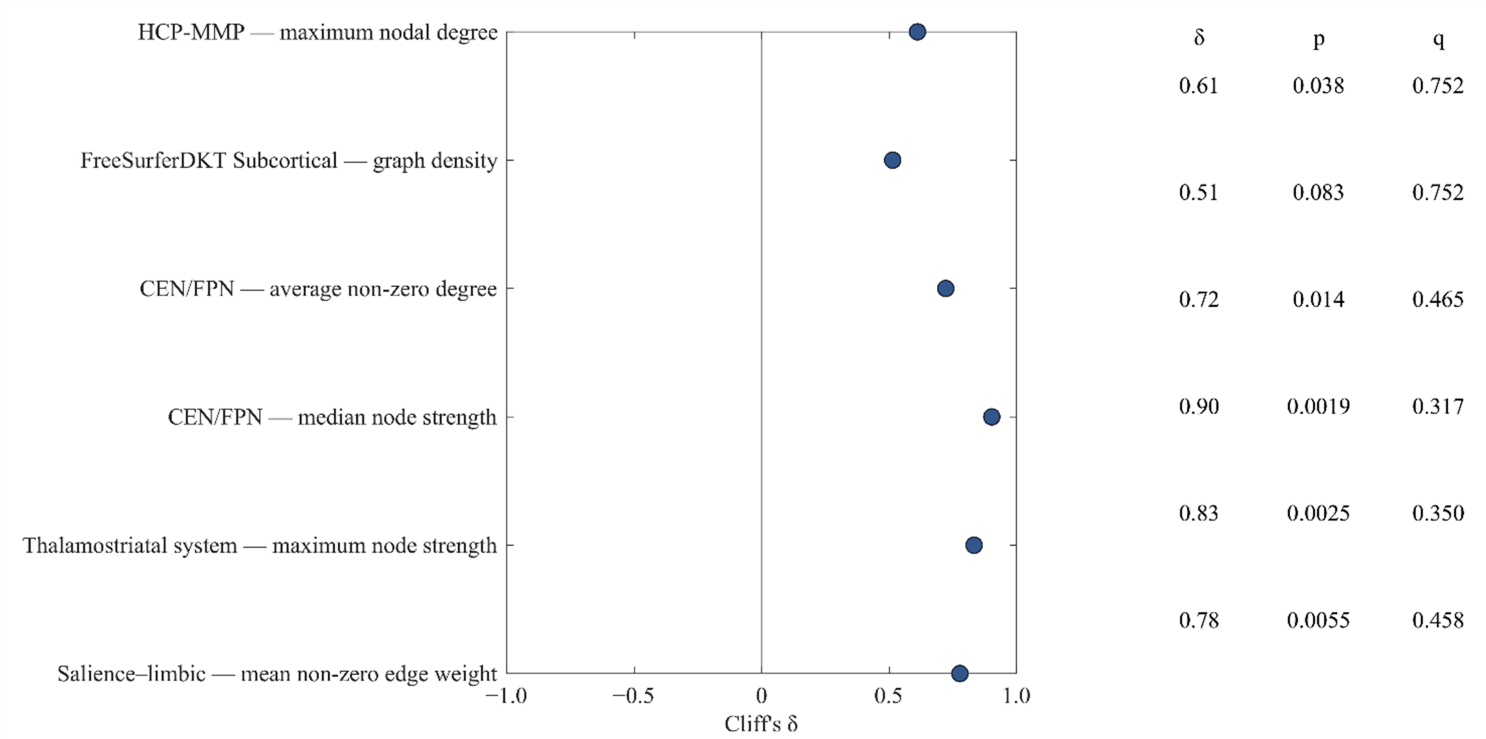


Figure 3

Principal between-group effect sizes across connectome analyses.

Cliff's δ effect-size estimates for six principal comparisons from the primary end-region workflow: HCP-MMP maximum nodal degree, FreeSurferDKT Subcortical graph density, Central Executive/Frontoparietal Network average non-zero degree and median node strength, thalamostriatal maximum node strength, and salience-limbic mean non-zero edge weight. Each point represents one effect-size estimate. The vertical line denotes Cliff's δ = 0; positive values indicate higher measures in controls, whereas negative values indicate higher measures in participants with asymptomatic temporomandibular disorder. The displayed columns report Cliff's δ, two-sided Mann-Whitney U-test p values, and Benjamini-Hochberg-adjusted q values calculated within the corresponding analysis family. Confidence intervals are not displayed.

Supplementary Files

This is a list of supplementary files associated with this preprint. Click to download.

- SupplementaryLegends.docx
- SupplementaryFigureS8.tif
- SupplementaryFigureS10.tif
- SupplementaryFigureS9.tif
- SupplementaryFigureS5.tif

- SupplementaryTablesS1S2GuideforReviewers.docx
- SupplementaryTableS2.xlsx
- SupplementaryTableS1.xlsx
- SupplementaryFigureS7.tif
- SupplementaryFigureS6.tif
- SupplementaryFigureS4.tif
- SupplementaryFigureS3.tif
- SupplementaryFigureS2.tif
- SupplementaryFigureS1.tif
- Deidentifiedparticipantlevelstructuralconnectivitymatrixdataset.zip